sciendo RIGA TECHNICAL UNIVERSITY *Electrical, Control and Communication Engineering*
ISSN 2255-9159 (online)
ISSN 2255-9140 (print)
2018, vol. 14, no. 2, pp. 125–133
doi: 10.2478/ecce-2018-0015
https://content.sciendo.com

Bi-Directional Position and Speed Estimation Algorithm for Sensorless Control of BLDC Motor

Mitesh B. Astik* (*Assistant Professor, A. D. Patel Institute of Technology, Gujarat, India*)
Praghnesh Bhatt (*Associate Professor, Pandit Deendayal Petroleum University, Gandhinagar, India*)
Bhavesh R. Bhalja (*Associate Professor, Indian Institute of Technology, Roorkee, India*)

***Abstract* – The observer design for estimation of back EMF to control the Brushless DC (BLDC) motor is proposed in this paper. Rotor position of the BLDC motor is estimated using the sequence of estimated back EMF. During speed reversal of motor, the actual and estimated values of speed fail to track the reference speed and if corrective action is not taken by the observer, the motor goes into the unstable region. To overcome this problem, the speed estimation algorithm is proposed for BLDC motor control during its speed reversal operation. Infinite Impulse Response (IIR) Butterworth first order low-pass filters are used in the observer for smoothing the estimated back EMFs of the BLDC motor. A new controller scheme based on Modified Hybrid Fuzzy PI (MHFPI) controller is proposed to control the speed of the BLDC motor. The effectiveness of the proposed method has been validated through simulations for different disturbances such as step changes in the reference speed and load torque of the motor and results are compared with the existing methods.**

***Keywords* – Brushless motor; Estimation; Sensorless control; MATLAB.**

I. INTRODUCTION

In the BLDC motor, position sensor presents numerous disadvantages, such as increase in machine size, reduction in reliability, higher value of noise, etc. In order to remove the position sensor from the BLDC motor, various methods have been proposed for its sensorless control [1]–[6]. In most of the proposed methods, the performance of motor gets deteriorated during transient state, low speed operating range and at the time speed reversal. The rotor position estimation error decreases the starting torque; consequently, it increases the time needed for start-up, especially in the direct torque control (DTC) of PM motors [7]. So, it is important that the rotor position estimation error be minimized.

Asaei and Rostami [8] presented an estimation method based on the variation in current due to the saturation of the stator core. The error in estimated rotor position is around 6° during starting. Stirban et al. [9] proposed a speed and position observer for sensorless control of PM BLDC motor using estimation of line-to-line PM flux linkage. In this method, the speed error is very high and the estimated rotor position error is around 3–4° electrical. Terzic and Jadric [10] proposed a speed and rotor position estimation method of a BLDC motor using extended Kalman filter. This method has very large estimated rotor position error for below rated speed of the motor. Rostami and Asaei [11] proposed a method for the initial rotor position estimation of PM motors based on the saturation effect. This method has the maximum estimated rotor position error of ±3.75°.

The rotor position can be determined from the $\alpha\beta$ components of back EMF [12]. Methods for constant current models of BLDC motor has been discussed in [13] to obtain good torque-speed characteristics.

Four Quadrant operation of the BLDC motor was explained in many papers for sensor based BLDC motor drive [14]–[16]. The direction of motor speed can be controlled from the position of the hall sensors. In sensorless operation of the BLDC motor drive, speed and position can be estimated with the help of the estimated back EMF.

The main objective of this paper is to develop a solution to control the dynamic behaviour of the BLDC motor and also to minimize the estimated rotor position error when it rotates in the reverse direction. When the motor rotates in the reverse direction, the behaviour of the motor is distorted and the motor may be dragged to unstable region. To overcome this problem, the speed estimation algorithm is proposed in this paper to control the dynamic behaviour of the motor in both the directions.

Nowadays, the Proportional Integral (PI) controllers have been commonly used but they are not suitable for non-linear and complex systems which can't be represented with the exact mathematical models. In such cases, fuzzy logic-based controller can be the better alternative of the PI controller. Shanmugasundram et al. in their paper [17] proposed design and implementation of a fuzzy controller for controlling the speed of the BLDC motor, in which the comparison between the fuzzy and PID controller has been presented. In recent years, a hybrid fuzzy logic controller was proposed for the induction motor, synchronous motor and BLDC motor drive [18]–[20], respectively.

In this paper, the back EMF of the BLDC motor is continuously estimated using an unidentified input observer. The rotor position is estimated using the sequence of estimated back EMF and with the help of the speed estimation algorithm. Infinite Impulse Response (IIR) Butterworth first order low-pass filters are used in an observer for smoothing the estimated back EMFs [21]. The Modified Hybrid Fuzzy PI (MHFPI) controller is used to control the speed of the motor. From simulation results reached in this paper, the maximum estimated rotor position error observed is less than 1° electrical.

* Corresponding authors.
E-mail: miteshastik@yahoo.com

II. Observer Design for BLDC Motor

The equation of the three phase voltages of the BLDC motor can be expressed as (1) [22], [23].

$$\begin{bmatrix} V_a \\ V_b \\ V_c \end{bmatrix} = \begin{bmatrix} R_s & 0 & 0 \\ 0 & R_s & 0 \\ 0 & 0 & R_s \end{bmatrix} \begin{bmatrix} i_a \\ i_b \\ i_c \end{bmatrix} + \begin{bmatrix} L & 0 & 0 \\ 0 & L & 0 \\ 0 & 0 & L \end{bmatrix} \frac{d}{dt} \begin{bmatrix} i_a \\ i_b \\ i_c \end{bmatrix} + \begin{bmatrix} e_a \\ e_b \\ e_c \end{bmatrix} \quad (1)$$

where V_a, V_b and V_c are the stator phase voltages, i_a, i_b and i_c are the stator phase currents, R_s and L are the stator per phase winding resistance and per phase winding inductance, respectively. e_a, e_b and e_c are the back EMFs of each phase.

The line-to-line voltage equations can be represented by (2).

$$v_z = R_s i_z + L\frac{di_z}{dt} + e_z \quad (2)$$

where z indicates line-to-line quantities of the BLDC motor.

Normally speed and position are measured with the use of sensors. Whereas the proposed approach estimates speed and position using back EMF estimation.

A. Back EMF Estimation

The time derivative of the stator current can be represented in (3) with the use of (2).

$$\dot{i}_z = -\frac{R_s}{L} i_z + \frac{1}{L} v_z - \frac{1}{L} e_z \quad (3)$$

The back EMF of the BLDC motor can be estimated using an unknown input observer [24]. The generalized estimation of back EMF for three-phase BLDC motor can be represented by (4).

$$\begin{bmatrix} \dot{\hat{i}}_z \\ \dot{\hat{e}}_z \end{bmatrix} = \begin{bmatrix} -\frac{R_s}{L} - g_1 & -\frac{1}{L} \\ -g_2 & 0 \end{bmatrix} \begin{bmatrix} \hat{i}_z \\ \hat{e}_z \end{bmatrix} + \begin{bmatrix} \frac{1}{L} \\ 0 \end{bmatrix} v_z + \begin{bmatrix} g_1 \\ g_2 \end{bmatrix} i_z \quad (4)$$

where g_1 and g_2 are the observer gains.

Solving (4), we have

$$\dot{\hat{e}}_z = g_2\left(i_z - \hat{i}_z\right) \quad (5)$$

If the gains of the observer are selected properly, this observer can accurately estimate line-to-line currents and back-EMFs of motor.

B. Rotor Speed Estimation

The estimated rotor speed ($\hat{\omega}_m$) is expressed as the ratio of estimated back EMF to torque constant and is given in (6).

$$\hat{\omega}_m = \frac{\hat{e}}{K_T} \quad (6)$$

where $\hat{e}$ is the absolute and maximum value of three estimated back EMFs, λ_p is the flux linkage established by magnets and P is the number of poles. Torque constant K_T is given by (7) [25].

$$K_T = \lambda_p * \left(P/2\right) \quad (7)$$

When the reference speed is positive, the actual and estimated speed successfully track the reference speed. On the other hand, they fail to track the reference speed when it becomes negative. During this situation, if corrective action is not taken by the observer, the motor goes into unstable region. This problem cannot be solved by using only (6). Therefore, to overcome this difficulty, the proposed algorithm is suggested to control the dynamic behaviour of the BLDC motor.

III. Proposed Algorithm for BLDC Motor

Fig. 1(a) shows the sequences of the estimated back EMFs for positive rotation from which the rotor's angular position can be decided. The rotor angle segment is to be found by comparing values of estimated line-to-line emfs $\hat{E}_{ab}$, $\hat{E}_{bc}$ and $\hat{E}_{ca}$ for positive rotation. For accurate zero crossing of the estimated back EMFs, the value of the estimated rotor's angular position for positive rotation $\hat{\theta}_{e+}$ can be found out from Table I. The near-linear portions of the trapezoidal waveform are used for robust estimation results.

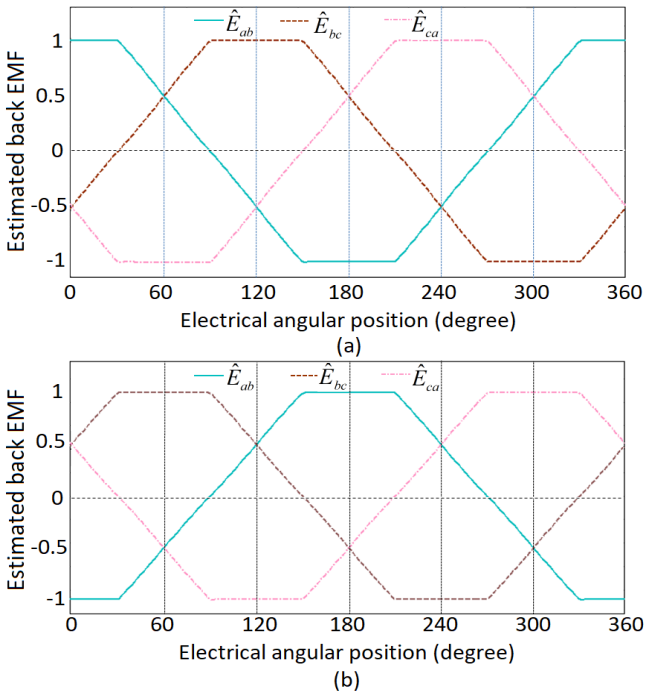

Fig. 1. Estimated back EMFs for (a) positive rotation and (b) negative rotation.

Fig. 1(b) shows the sequences of the estimated back EMFs for negative rotation. The exact value of the estimated rotor's angular position for negative rotation $\hat{\theta}_{e-}$ can be found out from Table II.

TABLE I

ESTIMATED BACK EMF SEQUENCE AND ELECTRICAL ANGULAR POSITION $\hat{\theta}_{e+}$ FOR POSITIVE ROTATION

Range of electrical angular position ($\hat{\theta}_{e+}$)	Estimated back EMF Sequence	$\hat{\theta}_{e+}$ Value for zero crossing Estimated back EMF
$0 \le \hat{\theta}_e < \frac{\pi}{3}$	$\hat{E}_{ab} > \hat{E}_{bc} \ge \hat{E}_{ca}$	$\frac{2\pi}{3} - \cos^{-1}\left(\hat{E}_{bc}\right)$
$\frac{\pi}{3} \le \hat{\theta}_e < \frac{2\pi}{3}$	$\hat{E}_{bc} \ge \hat{E}_{ab} > \hat{E}_{ca}$	$\cos^{-1}\left(\hat{E}_{ab}\right)$
$\frac{2\pi}{3} \le \hat{\theta}_e < \pi$	$\hat{E}_{bc} > \hat{E}_{ca} \ge \hat{E}_{ab}$	$\frac{4\pi}{3} - \cos^{-1}\left(\hat{E}_{ca}\right)$
$\pi \le \hat{\theta}_e < \frac{4\pi}{3}$	$\hat{E}_{ca} \ge \hat{E}_{bc} > \hat{E}_{ab}$	$\frac{2\pi}{3} + \cos^{-1}\left(\hat{E}_{bc}\right)$
$\frac{4\pi}{3} \le \hat{\theta}_e < \frac{5\pi}{3}$	$\hat{E}_{ca} > \hat{E}_{ab} \ge \hat{E}_{bc}$	$2\pi - \cos^{-1}\left(\hat{E}_{ab}\right)$
$\frac{5\pi}{3} \le \hat{\theta}_e < 2\pi$	$\hat{E}_{ab} \ge \hat{E}_{ca} > \hat{E}_{bc}$	$\frac{4\pi}{3} + \cos^{-1}\left(\hat{E}_{ca}\right)$

TABLE II

ESTIMATED BACK EMF SEQUENCE AND ELECTRICAL ANGULAR POSITION $\hat{\theta}_{e-}$ FOR NEGATIVE ROTATION

Range of electrical angular position ($\hat{\theta}_{e-}$)	Estimated back EMF sequence	$\hat{\theta}_{e-}$ Value for zero crossing estimated back EMF
$0 \le \hat{\theta}_e < \frac{\pi}{3}$	$\hat{E}_{bc} \ge \hat{E}_{ca} > \hat{E}_{ab}$	$\frac{2\pi}{3} - \cos^{-1}\left(-\hat{E}_{ca}\right)$
$\frac{\pi}{3} \le \hat{\theta}_e < \frac{2\pi}{3}$	$\hat{E}_{bc} > \hat{E}_{ab} \ge \hat{E}_{ca}$	$\cos^{-1}\left(-\hat{E}_{ab}\right)$
$\frac{2\pi}{3} \le \hat{\theta}_e < \pi$	$\hat{E}_{ab} \ge \hat{E}_{bc} > \hat{E}_{ca}$	$\frac{4\pi}{3} - \cos^{-1}\left(-\hat{E}_{bc}\right)$
$\pi \le \hat{\theta}_e < \frac{4\pi}{3}$	$\hat{E}_{ab} > \hat{E}_{ca} \ge \hat{E}_{bc}$	$\frac{2\pi}{3} + \cos^{-1}\left(-\hat{E}_{ca}\right)$
$\frac{4\pi}{3} \le \hat{\theta}_e < \frac{5\pi}{3}$	$\hat{E}_{ca} \ge \hat{E}_{ab} > \hat{E}_{bc}$	$2\pi - \cos^{-1}\left(-\hat{E}_{ab}\right)$
$\frac{5\pi}{3} \le \hat{\theta}_e < 2\pi$	$\hat{E}_{ca} > \hat{E}_{bc} \ge \hat{E}_{ab}$	$\frac{4\pi}{3} + \cos^{-1}\left(-\hat{E}_{bc}\right)$

The estimated back EMFs, which are derived in (5), consist of unwanted signals. To get exact rotor position, the estimated back EMFs should be smoothed by IIR Butterworth first order low-pass filters which have more sharpness with faster transition and lower pass band ripple in frequency response as compared to the same order of low-pass filters.

The estimated angular displacement $\Delta\hat{\theta}_e(k)$ is obtained by comparing $\hat{\theta}_e(k)$ and $\hat{\theta}_e(k-1)$ as given by (8) and is shown in Fig. 2.

$$\Delta\hat{\theta}_e(k) = \hat{\theta}_e(k) - \hat{\theta}_e(k-1) \tag{8}$$

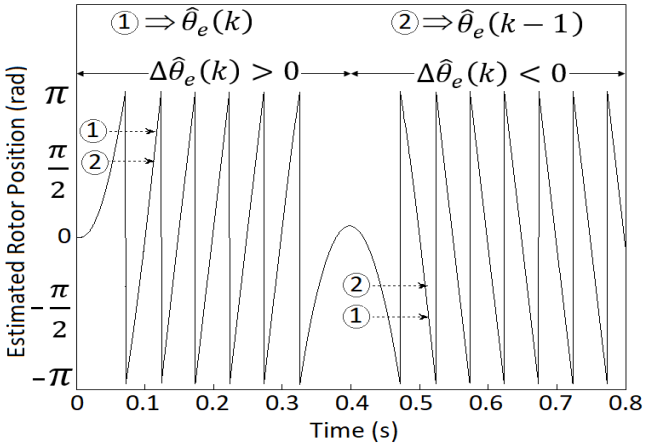

Fig. 2. Estimated rotor position for different step change in reference speed.

where $\hat{\theta}_e(k)$ and $\hat{\theta}_e(k-1)$ are present and the previous sampling instant of the estimated rotor position respectively, $\Delta\hat{\theta}_e(k)$ is the estimated angular displacement.

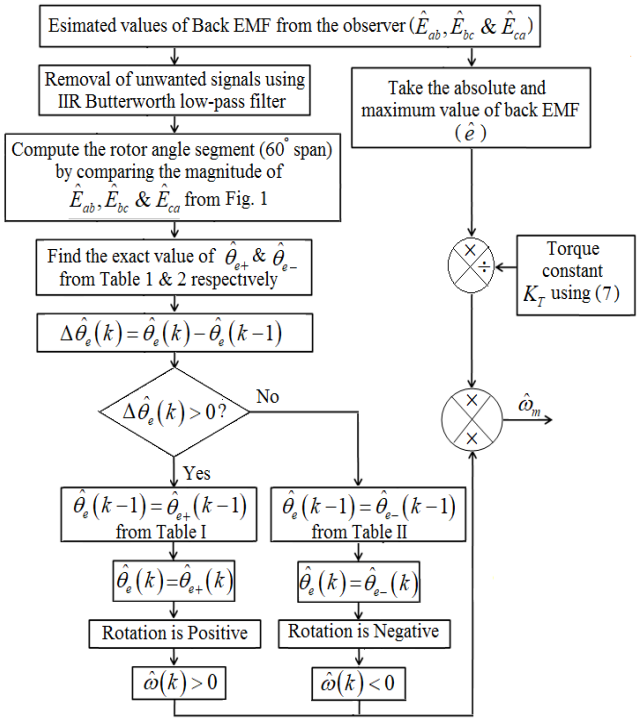

Fig. 3. Estimated speed algorithm for the BLDC motor.

Fig. 3 shows speed estimation algorithm for the BLDC motor, which is implemented in this paper. If the motor is rotating in positive direction, the estimated angular

displacement $\Delta\hat{\theta}_e(k)$ is greater than zero. Hence, the estimated rotor position $\hat{\theta}_e(k)$ follows the $\hat{\theta}_{e+}$ value of Table I and hence the speed direction is positive. If the rotor position is reversed, the estimated angular displacement $\Delta\hat{\theta}_e(k)$ is less than zero. Hence, the estimated rotor position $\hat{\theta}_e(k)$ follows $\hat{\theta}_{e-}$ value of Table II and hence the speed direction is negative.

Fig. 4 shows the block diagram of the proposed sensorless BLDC motor. $\omega_m^*(n)$ and $\hat{\omega}_m(n)$ are the reference speed and estimated speed of the motor, respectively. Commutation signals and DC-link voltage are used to calculate DC line voltage. Speed and position are calculated using the back EMF observer and the proposed estimated speed algorithm. The speed error is fed to the MHFPI controller which decides the current set value depending upon the gain values of the controller. A reference stator current I_s^* is found from the ratio of torque reference to torque constant K_T. The gate signals for inverter are generated by using commutation signals and comparing the actual and reference current through the hysteresis current controller. The gain of the hysteresis band controller used in this paper is 0.01 for better current control. For better estimation of the back EMF, the values of the observer gain g_1 and g_2 set in this paper are 3000 and –49500 respectively.

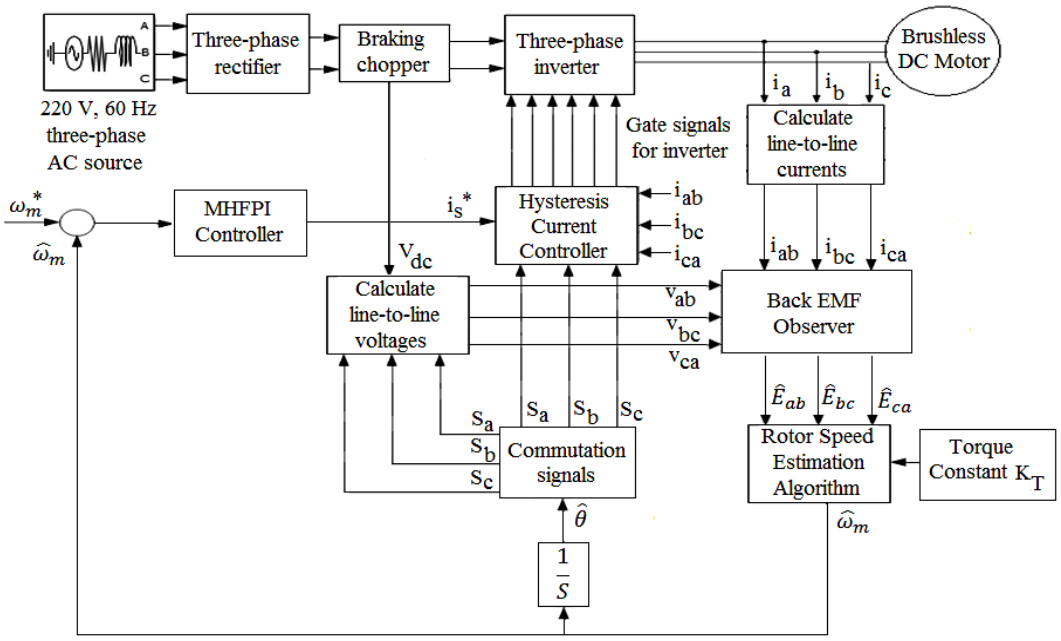

Fig. 4. Block diagram of the proposed sensorless BLDC motor.

IV. Modified Hybrid Fuzzy PI (MHFPI) Controller

The FLC has two inputs, error $\omega_e(n)$ and change of error $\Delta\omega_e(n)$, which are defined by

$$\omega_e(n) = \omega_m^*(n) - \hat{\omega}_m(n) \tag{9}$$

$$\Delta\omega_e(n) = \omega_e(n) - \omega_e(n-1) \tag{10}$$

Indexes n and (n-1) indicate the present state and the previous state of the speed, respectively. The output of the FLC is the incremental change in the control signal $\Delta u(n)$. Membership function of the FLC input $\omega_e(n)$ is normalized between [−15, 15], $\Delta\omega_e(n)$ is normalized between [$-1e^6$, $1e^6$] and the output $\Delta u(n)$ is normalized between [−25, 25].

Parallel Fuzzy PI (PFPI) controller is the addition to the PI and fuzzy controller. The combination of PI and Parallel Fuzzy PI (PFPI) controller is used as a MHFPI controller. The objective of this controller is to produce better response than the conventional controllers. Two switching functions for the MHFPI controller have been considered. An approach for the switching control for this controller is such that for most of the time the PI controller is activated and use of the PFPI controller only when the system behaviour is oscillatory or tends to overshoot. The selection between the PI and PFPI controller is based on the following condition:

- if the error signal $\omega_e(n)$ is strictly greater than zero and its previous value $\omega_e(n-1)$ was strictly less than or equal to zero, the PI controller will work;
- if the previous value of error signal is strictly greater than zero, the PFPI controller will work.

$$U_{MHFPI} = \begin{cases} U_{PI}, \text{ for } \omega_e(n-1) \le 0 \text{ and } \omega_e(n) > 0 \\ U_{PFPI}, \text{ for } \omega_e(n-1) > 0 \text{ and all } \omega_e(n) \end{cases} \tag{11}$$

V. Simulation Results and Discussions

To validate the effect of the observer, proposed algorithm and controller, various simulations have been carried out on the BLDC motor under variations in speed and load.

The parameters of the BLDC motor used for MATLAB simulation are shown in Table III.

TABLE III
BLDC MOTOR PARAMETERS

Parameters	Ratings
Stator resistance (R_s)	0.2 Ω
Stator inductance (L)	8.5 mH
Rotor inertia (J)	89×10^{-3} kg-m^2
Friction (B)	5×10^{-3} Nm-s
Number of pole pair (p)	4
Rated speed (ω_s)	300 rpm
Flux linkage established by magnets (λ_p)	0.175 (volt-s)

Fig. 5 shows dynamic responses of speed, torque, estimated line-to-line back EMF and rotor position for different step changes in reference speed with zero load torque.

The step change in reference speed is applied from zero to 300 rpm at t = 0 s, the motor speed and subsequently the estimated back EMFs start increasing and attain the steady state value within 0.1 s. Again, the disturbance is applied in reference speed from steady state speed to −300 rpm at t = 0.3 s. It is observed from Fig. 5 that motor speed smoothly decreases from 300 rpm to 0 rpm, but it shows peculiar response after crossing zero rpm and starts rotating in the negative direction. The motor fails to attain the reference speed for this negative step change. The application of the proposed algorithm can successfully solve this problem.

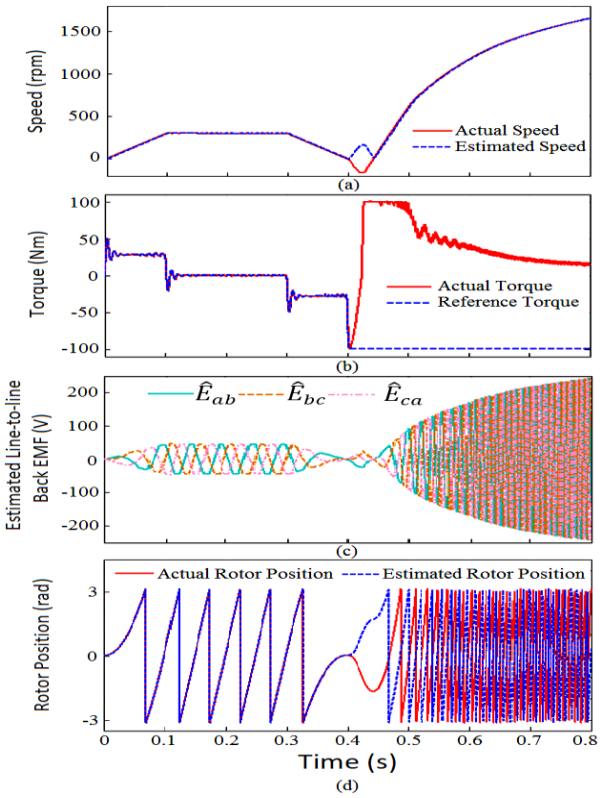

Fig. 5. Dynamic response of the BLDC motor for different step changes in reference speed.

To validate the effectiveness of the proposed algorithm, two types of disturbances (i) step change in reference speed keeping load torque zero and (ii) step change in load torque with different reference speed are considered. The simulation results for these disturbances with the proposed algorithm are presented in the subsequent section.

A. Step Change in Reference Speed Keeping Load Torque Zero

The variations in speed, torque and Zero Crossing Point (ZCP) for the estimated back EMF, estimated rotor position and estimated commutation signal are shown in Figs. 6 to 8 following the step change in reference speed from 300 rpm to −300 rpm, 100 rpm to −100 rpm and 500 rpm to −500 rpm, respectively. From Fig. 6, it can be observed that the motor performance remains the same up to 0.3 s, which was discussed in Fig. 5. The motor can successfully attain the reference speed of −300 rpm at t = 0.5 s even in negative direction of rotation. This shows the effectiveness of the proposed algorithm that makes the operation of the motor possible even in reverse direction of rotation, which could not be the case earlier as shown in Fig. 5.

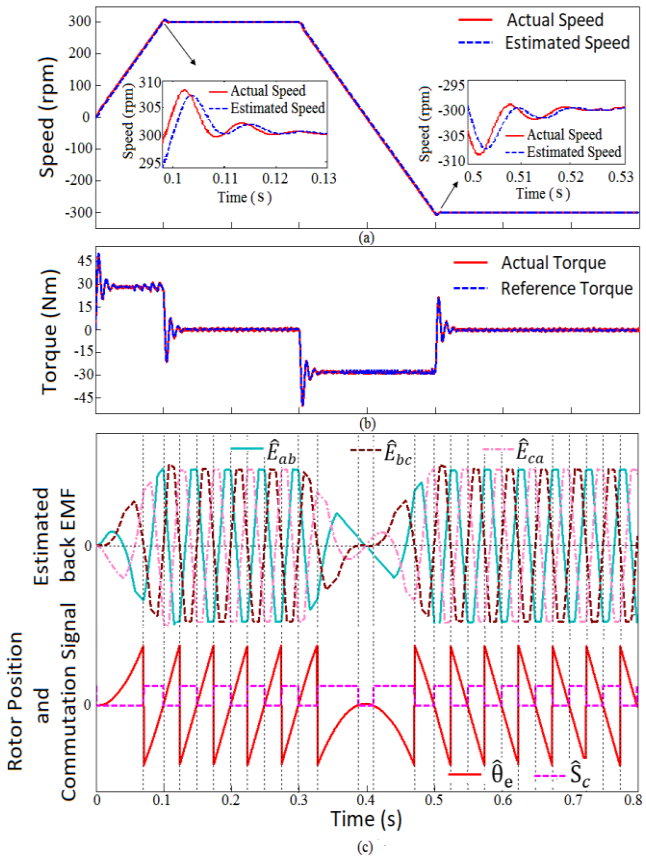

Fig. 6. Dynamic response of (a) speed (b) torque and (c) ZCP of back EMF, rotor position and commutation signal for step change in speed from 300 rpm to −300 rpm.

Similar effects can be seen in Figs. 7 and 8 when the disturbance in reference speed is applied when the motor operates at below and above rated speed, respectively. The comparison between actual and estimated speed is shown in Figs. 6(a), 7(a) and 8(a) for all three different cases under considerations. The results obtained from the observer design

show negligible error between actual and estimated speed during the steady state. These errors during transient period do not exceed beyond 1.7 %, 5 % and 1 % while motor operates at rated, below rated and above rated speed, respectively.

MHFPI controller successfully limits the overshoot in speed during the transient period and suppresses the oscillations as quickly as possible. Accurate tracking of actual torque and reference torque is also achieved during forward as well as reverse rotation of the motor as shown in Figs. 6(b), 7(b) and 8(b).

The change in phase sequence of the estimated back EMFs and the rotor position can be clearly observed from Figs. 6(c), 7(c) and 8(c) with the rotation of the motor in the negative direction, which follows the discussion of Fig. 1 (b). In this paper, ideal commutation points are obtained from the line-to-line estimated back EMFs. The obtained ZCPs are inherently in phase with the estimated commutation signals as well as the estimated rotor position. It can be seen that the commutation is occurred when the estimated back EMF of phase 'bc' is crossing zero and the remaining two lines estimated back EMFs have the same magnitude but different direction.

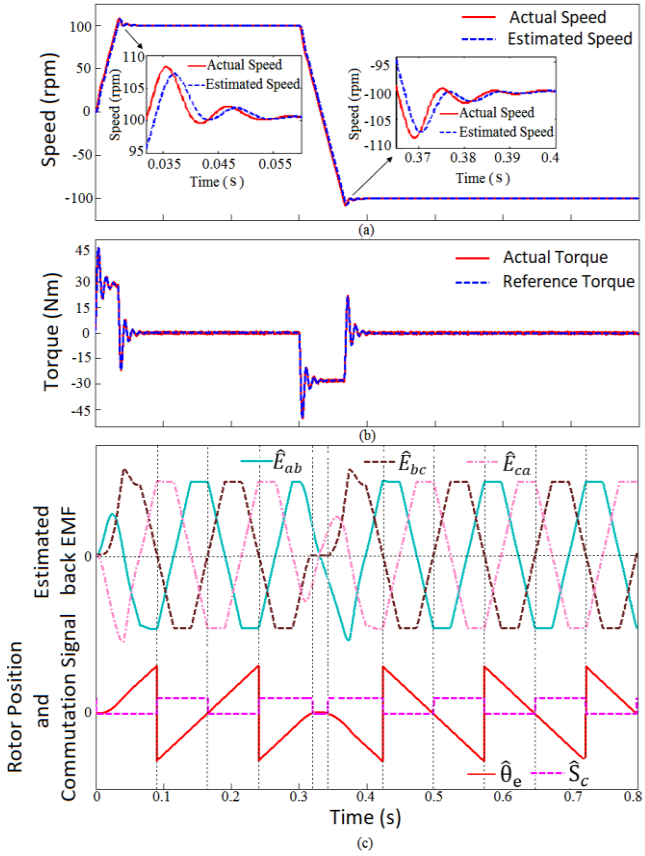

Fig. 7. Dynamic response of (a) speed (b) torque and (c) ZCP of back EMF, rotor position and commutation signal for step change in speed from 100 rpm to −100 rpm.

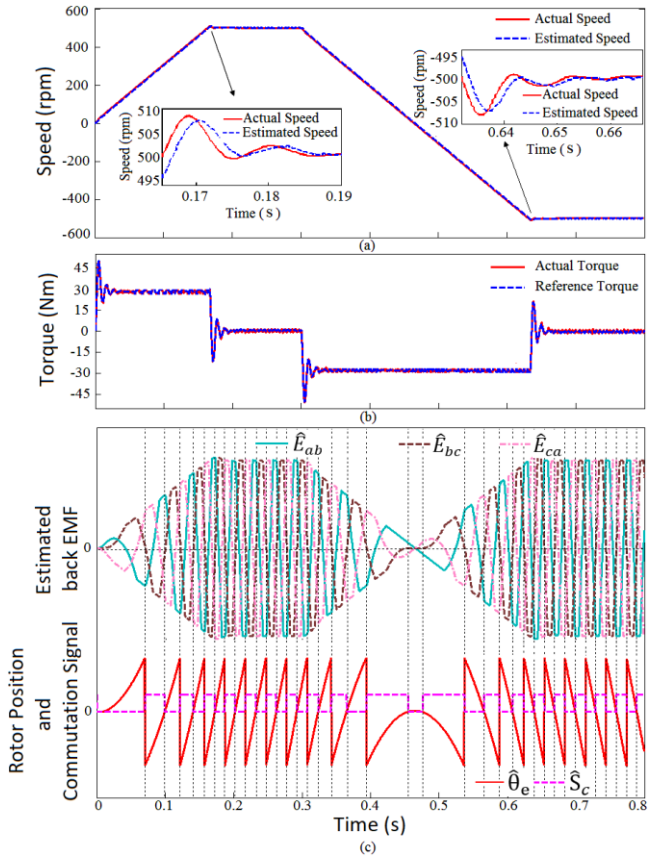

Fig. 8. Dynamic response of (a) speed (b) torque and (c) ZCP of back EMF, rotor position and commutation signal for step change in speed from 500 rpm to −500 rpm.

B. Step Change in Load Torque with Different Reference Speed

Figs. 9 to 11 show the dynamic response of speed, torque and ZCPs for the estimated back EMF, estimated rotor position and the estimated commutation signal for three different speeds. In Fig. 9, the motor behaviour is the same as discussed in the previous subsection up to 0.3 s. Now the disturbance is applied in load torque from no-load to 10 N m at t = 0.3 s keeping reference speed at 300 rpm constant. At this instant, the motor's actual and estimated speeds are reduced around 3 rpm and the motor attains the reference speed again within 0.03 s to 0.04 s, which can be seen from Fig. 9 (a). Again, the disturbance is applied in load torque from 10 N m to −10 N m at t = 0.5 s, the motor speed slightly increases and again attains the reference speed within the short time. Similar effects can be seen in Figs. 10 and 11 when the motor operates at below and above rated speed, respectively. The comparison between actual and estimated speed is shown in Figs. 9(a), 10(a) and 11(a) for three different cases under considerations.

Accurate tracking of the actual torque and reference torque is also achieved during transient as well as steady state for all three cases, as shown in Figs. 9(b), 10(b) and 11(b), respectively. As the variation in the motor speed is very low, the actual and estimated back EMFs are almost constant in steady state throughout the simulation.

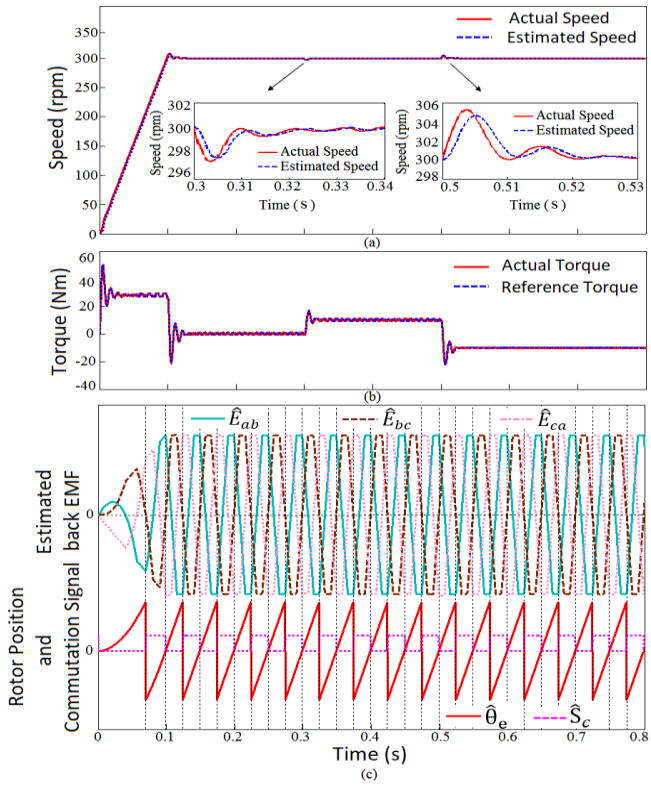

Fig. 9. Dynamic response of (a) speed (b) torque and (c) ZCP of back EMF, rotor position and commutation signal for step change in load torque from no-load to 10 Nm and from 10 N m to −10 N m with reference speed set at 300 rpm.

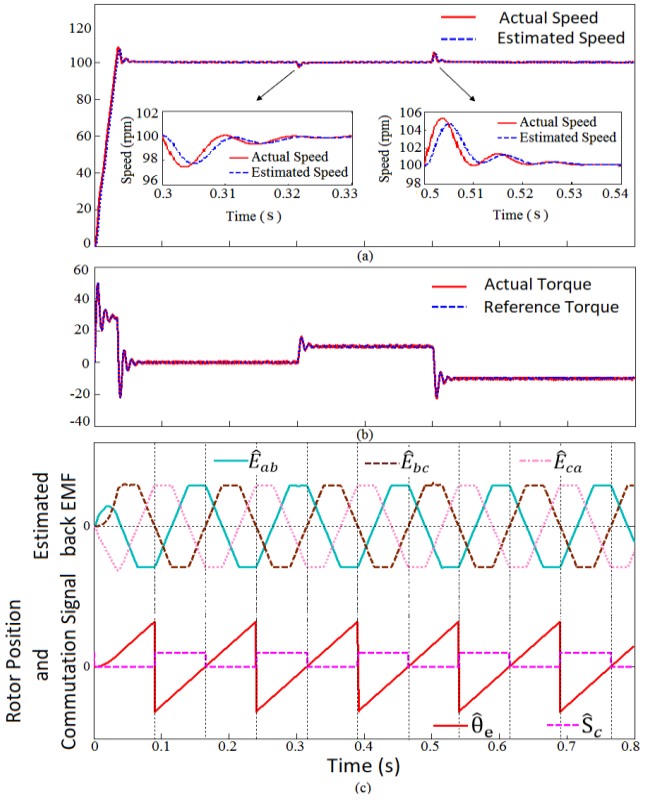

Fig. 10. Dynamic response of (a) speed (b) torque and (c) ZCP of back EMF, rotor position and commutation signal for step change in load torque from no-load to 10 N m and from 10 N m to −10 N m with reference speed set at 100 rpm.

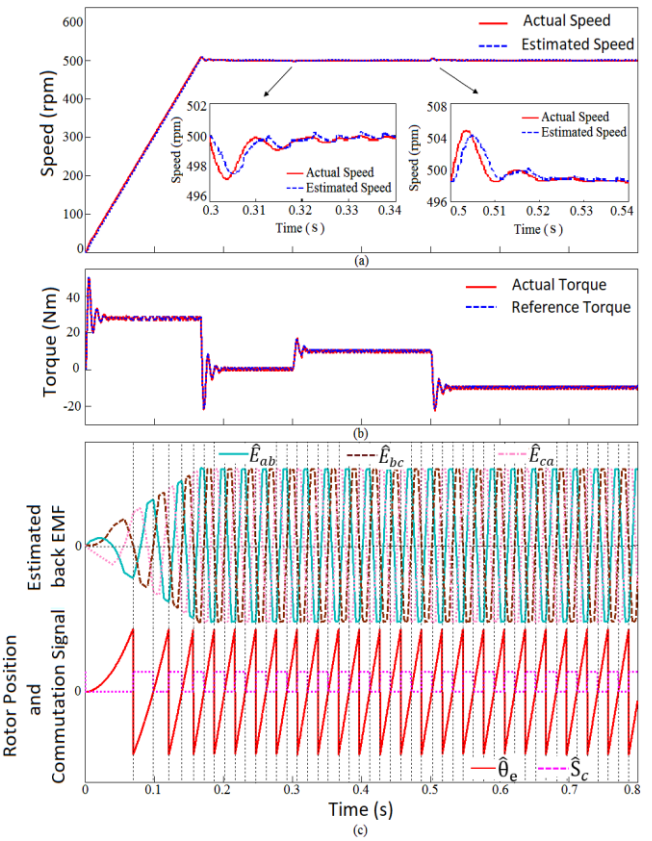

Fig. 11. Dynamic response of (a) speed (b) torque and (c) ZCP of back EMF, rotor position and commutation signal for step change in load torque from no-load to 10 N m and from 10 N m to −10 N m with reference speed set at 500 rpm.

From Figs. 9(c), 10(c) and 11(c), the phase sequence of the back EMFs and rotor position is same as motor is rotating in forward direction. Moreover, the obtained ZCPs are inherently in phase with the estimated commutation signals as well as estimated rotor position.

C. Comparative Evaluation of the Proposed Scheme with the Existing Schemes

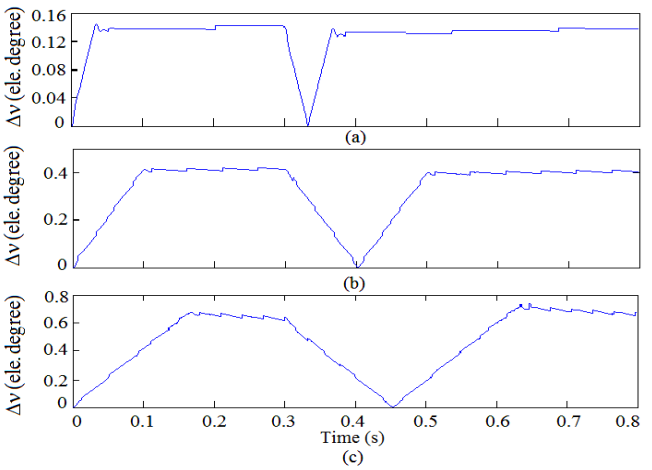

Fig. 12. Estimated rotor position error on no-load when step change in speed from (a) 100 rpm to −100 rpm (b) 300 rpm to −300 rpm and (c) 500 rpm to −500 rpm.

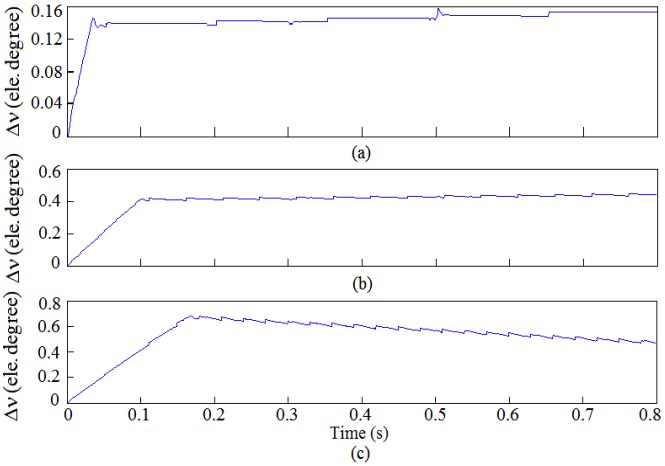

Fig. 13. Estimated rotor position error when step change in load torque from no-load to 10 N m and from 10 N m to −10 N m with reference speed set at (a) 100 rpm (b) 300 rpm and (c) 500 rpm.

From Fig. 12, it is observed that the estimated rotor position error is 0.15°, 0.42° and 0.7° electrical for step change in reference speed from 100 rpm to −100 rpm, 300 rpm to −300 rpm and 500 rpm to −500 rpm, respectively, for no-load condition. From Fig. 13, it can be seen that the estimated rotor position error is 0.155°, 0.45° and 0.7° electrical for below rated, rated and above rated speed, respectively, when step change in load from no-load to 10 N m and from 10 N m to −10 N m is applied.

The rotor position estimation error decreases the starting torque; consequently, it increases the time needed for start-up, especially in the direct torque control (DTC) of PM motors [7]. So, it is important that the rotor position estimation error be minimized. Comparative evaluation of the proposed scheme has been carried out with the existing schemes [8]–[11] in terms of the estimated rotor position error. An estimation method based on the variation in current due to the saturation of the stator core is presented in [8]. It is observed from Fig. 10 of existing scheme [8] that the estimated rotor position error is around 6° electrical during starting. Speed and position observer for sensorless control of PM BLDC motor using estimation of line-to-line PM flux linkage has been discussed in [9]. The speed error is very large and estimated rotor position error is around 3– 4° electrical, which is observed from Fig. 10 of existing scheme [9]. The speed and rotor position of BLDC motor are estimated in [10] using extended Kalman filter. It can be seen from Fig. 7 of existing scheme [10] that the estimated rotor position error is very large and is around 12–16° electrical for below rated speed of the motor. The initial rotor position estimation of PM motors based on saturation effect has been proposed in [11]. The maximum estimated rotor position error is ±3.75° electrical which is mentioned in Table I of the existing scheme [11]. Conversely, from Fig. 12 and Fig. 13 of this paper, it can be seen that the error given by the proposed scheme is less than 1° electrical during transient as well as steady state conditions for all speed variations (below rated, rated and above rated speed) even with no-load/full load situation. This shows the effectiveness of the speed estimation algorithm, controller and observer design.

VI. Conclusion

This paper presents an approach for sensorless control of the BLDC motor using an unidentified input observer. The rotor position is estimated using the sequence of estimated back EMF and with the help of speed estimation algorithm without any additional hardware. It is observed that without using the proposed algorithm, the motor goes into unstable region during reversal of the motor speed. Hence, a speed estimation algorithm is proposed to get better performance even in reverse rotation of the BLDC motor. The obtained ZCPs of the estimated back EMFs are inherently in phase with the estimated commutation signals as well as the estimated rotor position. From simulation results, it is concluded that the proposed algorithm, controller and observer satisfactorily work in both rotational directions and the error between actual and estimated rotor position is less than 1° electrical in transient as well as in steady state conditions. The obtained results have been validated for rated, below rated and above rated speed of BLDC motor under different loading conditions.

References

[1] C.-T. Lin, C.-W. Hung and C.-W. Liu, “Sensorless Control for Four-Switch Three-Phase Brushless DC Motor Drive”, *Conf. Rec. 2006 IEEE Industry Applications Conference Forty-First IAS Annual Meeting*, pp. 2048–2053, 2006. https://doi.org/10.1109/IAS.2006.256817

[2] J. X. Shen, Z. Q. Zhu and D. Howe, “Sensorless Flux-Weakening Control of Permanent-Magnet Brushless Machines Using Third Harmonic Back EMF”, *IEEE Trans. Ind. Appl.*, vol. 40, no. 6, pp. 1629–1636, 2004. https://doi.org/10.1109/TIA.2004.836157

[3] J. X. Shen and S. Iwasaki, “Sensorless Control of Ultrahigh-Speed PM Brushless Motor Using PLL and Third Harmonic Back EMF”, *IEEE Trans. Ind. Electron.*, vol. 53, no. 2, pp. 421–428, 2006. https://doi.org/10.1109/TIE.2006.870664

[4] S. Ogasawara and H. Akagi, “An Approach to Position Sensorless Drive for Brushless DC Motors”, *IEEE Trans. Ind. Appl.*, vol. 27, no. 5, pp. 928–933, 1991. https://doi.org/10.1109/28.90349

[5] X. Z. Zhang and Y. N. Wang, “A Novel Position-Sensorless Control Method for Brushless DC Motors”, *Energy Conversion and Management*, vol. 52, no. 3, pp. 1669–1676, 2010. https://doi.org/10.1016/j.enconman.2010.10.030

[6] T-W. Chun, Q-V. Tran, H.-H. Lee, H.-G. Kim, “Sensorless Control of BLDC Motor Drive for an Automotive Fuel Pump Using a Hysteresis Comparator”, *IEEE Trans. Power Electron.*, vol. 29, no. 3, pp. 1382–1391, 2014. https://doi.org/10.1109/TPEL.2013.2261554

[7] H. Ghassemi and S. Vaez-Zadeh, “A Very Fast Direct Torque Control for Interior Permanent Magnet Synchronous Motors Startup”, *Energy Conversion and Management*, vol. 46, no. 5, pp. 715–726, 2005. https://doi.org/10.1016/j.enconman.2004.05.005

[8] B. Asaei and A. Rostami, “A Novel Starting Method for BLDC Motors Without the Position Sensors”, *Energy Conversion and Management*, vol. 50, no. 2, pp. 337–343, 2008. https://doi.org/10.1016/j.enconman.2008.09.020

[9] A. Stirban, I. Boldea, and G. D. Andreescu, “Motion Sensorless Control of BLDC-PM Motor with Offline FEM Information Assisted Position and Speed Observer”, *IEEE Trans. Ind. Appl.*, vol. 48, no. 6, pp. 1950–1958, 2012. https://doi.org/10.1109/TIA.2012.2226194

[10] B. Terzic and M. Jadric, “Design and Implementation of the Extended Kalman Filter for the Speed and Rotor Position Estimation of Brushless DC Motor”, *IEEE Trans. Ind. Electron.*, vol. 48, no. 6, pp. 1065–1073, 2001. https://doi.org/10.1109/41.969385

[11] A. Rostami and B. Asaei, “A Novel Method for Estimating the Initial Rotor Position of PM Motors Without the Position Sensor”, *Energy Conversion and Management*, vol. 50, no. 8, pp. 1879–1883, 2009. https://doi.org/10.1016/j.enconman.2009.04.029

[12] S. M. Kazraj, R. B. Soflayi and M. B. B. Sharifian, "Sliding-Mode Observer for Speed and Position Sensorless Control of Linear-PMSM", *Electrical, Control and Communication Engineering*, vol. 5, no. 1, pp. 20–26, 2014. https://doi.org/10.2478/ecce-2014-0003

[13] K. Krykowski and J. Hetmanczyk, "Constant Current Models of Brushless DC Motor", *Electrical, Control and Communication Engineering*, vol. 3, no. 1, pp. 19–24, 2013. https://doi.org/10.2478/ecce-2013-0010

[14] M. V. Ramesh, G. S. Rao, J. Amarnath, S. Kamakshaiah and B. Jawaharlal, "Speed torque characteristics of brushless DC motor in either direction on load using ARM controller", *IEEE PES conference on Innovative Smart Grid Technologies*, pp. 217–222, Dec. 2011. https://doi.org/10.1109/iset-india.2011.6145385

[15] D. Das, N. Kumaresan, V. Nayanar, K. N. Sam and N. A. Gounden, "Development of BLDC Motor-Based Elevator System Suitable for DC Microgrid", *IEEE/ASME Transactions on Mechatronics*, vol. 21, no. 3, pp. 1552–1560, June 2016. https://doi.org/10.1109/TMECH.2015.2506818

[16] S. K. Awaze, "Four quadrant operation of BLDC motor in MATLAB/SIMULINK", *IEEE International Conference on Computational Intelligence and Communication Networks*, pp. 569–573, Sept. 2013. https://doi.org/10.1109/CICN.2013.124

[17] R. Shanmugasundram, K. M. Zakariah and N. Yadaiah, "Implementation and performance analysis of digital controllers for brushless DC motor drives", *IEEE/ASME Trans. Mechatronics*, vol. 19, no. 1, pp. 213–224, 2014. https://doi.org/10.1109/TMECH.2012.2226469

[18] M. Zerikat and S. Chekroun, "Design and Implementation of a Hybrid Fuzzy Controller for a High-Performance Induction Motor", *International Journal of Computer and Information Engineering*, vol. 1, no. 2, pp. 202–208, 2007. https://doi.org/10.5281/zenodo.1333794

[19] A. V. Sant and K. R. Rajagopal, "PM Synchronous Motor Speed Control Using Hybrid Fuzzy-PI with Novel Switching Functions", *IEEE Trans. on Magnetics*, vol. 45, no. 10, pp. 4672–4675, 2009. https://doi.org/10.1109/TMAG.2009.2022191

[20] A. Rubaai, D. Ricketts and M. D. Kankam, "Experimental Verification of a Hybrid Fuzzy Control Strategy for a High-Performance Brushless DC Drive System", *IEEE Trans. Ind. Appl*., vol. 37, no. 2, pp. 503–512, 2001. https://doi.org/10.1109/28.913715

[21] M. T. DiRenzo, "Switched Reluctance Motor Control – Basic Operation and Example Using the TMS320F240", Texas Instruments, SPRA420A Application Report, Digital Signal Processing Solutions, 2000.

[22] D.-H. Lee et al., "A Current Ripple Reduction of a High-Speed Miniature Brushless Direct Current Motor Using Instantaneous Voltage Control", *IET Electric Power Applications*, vol. 3, no. 2, pp. 85–92, 2009. https://doi.org/10.1049/iet-epa:20070490

[23] C.-L. Xia, *Permanent Magnet Brushless DC Motor Drives and Controls*. Singapore: John Wiley & Sons Ltd., 2012.

[24] T.-S. Kim, B.-G. Park, D.-M. Lee, Ji-Su Ryu and D.-S. Hyun, "A New Approach to Sensorless Control Method for Brushless DC Motors", *International Journal of Control, Automation and Systems*, vol. 6, no. 4, pp. 477–487, 2008.

[25] J.-W. Park, S.-H. Hwang and J.-M. Kim, "Sensorless Control of Brushless DC Motors with Torque Constant Estimation for Home Appliances", *IEEE Trans. Ind. Appl.*, vol. 48, no. 2, pp. 677–684, 2012. https://doi.org/10.1109/TIA.2011.2181774

Mitesh B. Astik was born in 1980 in Gujarat, India. He received the B.E. degree in Electrical Engineering from B.V.M. Engineering College, Sardar Patel University, Gujarat, India, in 2003, the M.E. degree in Electrical Engineering with specialization in control system from Veermata Jijabai Technological Institute, Mumbai University, Maharashtra in 2006. He is currently working toward the Ph.D. degree at C.S. Patel Institute of Technology, CHARUSAT, Changa, Gujarat, India. Since 2008, he has been with the Department of Electrical Engineering, A.D. Patel Institute of Technology, Gujarat, India. He has published five papers in journals and conferences at international and national levels. His research interests lie in the areas of electrical machines and electrical control systems. Mr. Astik is a life member of the Institution of Engineers (IE) India and Indian Society of Technical Education (ISTE).

Postal address: A.D. Patel Institute of Technology, Department of Electrical Engineering, New Vallabh Vidyanagar, Vitthal Udyognagar, Anand, Gujarat 388121, India.
E-mail: miteshastik@yahoo.com
ORCID ID: https://orcid.org/0000-0002-0141-143X

Dr. **Praghnesh Bhatt** is presently working as an Associate Professor in Department of Electrical Engineering, School of Technology of Pandit Deendayal Petroleum University (PDPU), Gandhinagar. He completed his B.E. in Electrical Engineering from L D College of Engineering, Ahmedabad and M.E. in Electrical Engineering from BVM Engineering College, Vallabh Vidhyanagar with specialization in Electrical Power Systems. He received his PhD from S V National Institute of Technology (SVNIT), Surat in year 2012. He has published many research papers in globally reputed international journals and conferences. He is a member of IEEE and IEEE Power & Energy Society. He is also a life member of Indian Society of Technical Education (ISTE). His areas of interest are Power System Dynamics and Stability, Grid Integration of Wind Power Generation, Distributed Generation, Smart Grid and Power System Protection.

Postal address: School of Technology, Department of Electrical Engineering, Pandit Deendayal Petroleum University, Raisan, Gandhinagar, Gujarat 382007, India.
E-mail: praghnesh.bhatt@sot.pdpu.ac.in
ORCID ID: https://orcid.org/0000-0002-0262-9991

Bhavesh R. Bhalja (M'2007-SM' 2010) received B. E. (Electrical Engineering) and M. E. degree in power system engineering from B.V.M. Engineering College, Sardar Patel University, Vallabh Vidyanagar, India, in 1999 and 2001, respectively. He obtained Ph. D from Indian Institute of Technology Roorkee in 2007. He has teaching experience of more than 17 years. Previously, he worked as an Associate Professor at Pandit Deendayal Petroleum University, Gandhinagar, Gujarat. Currently, he is working as an Associate Professor, Department of Electrical Engineering, Indian Institute of Technology Roorkee, Roorkee, India.
He has published more than 100 papers in journals at international and national levels. He was awarded Young Engineers Award by Institution of Engineers, India, in 2009. He was awarded "Certificate of Merit Award" by Institution of Engineers, India, in 2007. He was awarded "Hari-ohm Ashram Prerit Inter-University Smarak Trust Award" by Sardar Patel University, Vallabh Vidyanagar, Anand, India, in 2009. One of his papers titled "Miscordination of Relay in Radial Distribution Network Containing Distributed Generation" also got Best Poster award at IEEE Conference on Recent Advances in Intelligent Computational Systems, Sep 22–24, 2011, Trivandrum, India**.** Presently, he is on a sabbatical leave for availing Fulbright Fellowship as a visiting scholar at the Department of Electrical and Computer Engineering, Texas A&M University, College Station, Texas, USA for a period of nine months. He is also involved in many research and development projects of the Department of Science & Technology, Ministry of Science & Technology, and the Government of India. His research interests include Digital Protection & Automation, Smart Grid Technologies and Applications, Distributed Generation, Micro-grid, Power Quality Improvement, and Application of Artificial Intelligence.
Dr. Bhalja has supervised more than 50 UG projects, 15 M. Tech. Dissertations, 6 Ph. D students. He is a Senior Member of IEEE and Member of IE and ISTE.

Postal address: Indian Institute of Technology, Roorkee - Haridwar Highway, Roorkee, Uttarakhand 247667, India.
Email: bhaveshbhalja@gmail.com
ORCID ID: https://orcid.org/0000-0002-6289-7146